Minerals Engineering, Volume 15, Issue 11S1, pp.985-991.
(Presented at Pyromet '02, Cape Town, 11-12 March 2002.)

DC ARC PHOTOGRAPHY AND MODELLING

R.T. JONES[§], Q.G. REYNOLDS[§] and M.J. ALPORT[¶]

§ Pyrometallurgy Division, Mintek, Private Bag X3015, Randburg, 2125, South Africa
E-mail: rtjones@global.co.za
¶ Applied Physics Group, School of Pure and Applied Physics, University of Natal, South Africa

ABSTRACT

DC arc furnaces operate with a graphite cathode positioned above a molten slag and metal bath contained inside a furnace vessel. The plasma arc, consisting of ionised particles at extremely high temperatures, forms a conducting path between the graphite cathode and the molten bath. The power provided by the arc can be controlled by adjusting the arc length and the current.

The high-intensity plasma arc emanates from a relatively small attachment area on the graphite electrode, and extends down to the surface of the molten bath. Photographs of the arc are presented and compared to models of the shape of the arc. These models provide a description of how the arc voltage varies as a function of arc length and current, for a given set of conditions in the furnace.

The arc attachment zone, where the arc impinges on the molten slag surface, is highly turbulent and operates at a very high temperature. This promotes very rapid melting, fast reaction kinetics, and effective mixing. The impingement of the arc causes a crater-like depression in the surface of the slag. This has a significant effect on the distribution of current in the molten slag, and the voltage drop across the slag. The shape and size of this depression has been photographed, and the resulting information used in a model of the depression.

Keywords
Pyrometallurgy; extractive metallurgy; modelling

INTRODUCTION

The inherent persistency and intensity of a direct-current (DC) plasma arc offers some unique advantages for a number of smelting processes (Jones *et al*., 1993). DC arc furnaces operate with a graphite cathode positioned above a molten slag and metal bath contained inside a furnace vessel. The plasma arc, consisting of ionised particles at extremely high temperatures, forms a conducting path between the graphite cathode and the molten bath. At temperatures above about 5000 K, the constituent molecules of the gas ionise into positively charged ions and negatively charged electrons, giving a neutral but very strongly conductive plasma. This conducting material permits electrical current to pass from the furnace electrode through to the furnace bath and complete the circuit. Flow of the plasma in the arc column is driven very strongly downward by electromagnetic forces, in a jet from the electrode towards the molten bath. Much of the energy from the arc is delivered to a localised area directly beneath the arc, making this a very effective way of heating the process material. The power provided by the arc can be controlled by adjusting the arc length and the current.

The open arc provides an additional degree of freedom to the supply of energy to the furnace, in that the resistivity of the slag is no longer solely responsible for the dissipation of energy to heat the molten slag. This renders the energy supply nearly independent of slag composition, which may allow the slag chemistry to be optimized for the best recovery of valuable metals (instead of for the required electrical characteristics).

The high-intensity plasma arc emanates from a relatively small attachment area on the graphite electrode, and extends down to the surface of the molten bath. Photographs of the arc have been compared to models of its shape. These models provide a description of how the arc voltage varies as a function of arc length and current, for a given set of conditions in the furnace.

The arc attachment zone, where the arc impinges on the molten slag surface, is highly turbulent and operates at a very high temperature. This promotes very rapid melting, fast reaction kinetics, and effective mixing. The

impingement of the arc causes a crater-like depression in the surface of the slag. This is believed to have a significant effect on the distribution of current and temperature in the molten slag, and the voltage drop across the slag. The shape and size of this depression has been photographed, and the resulting information used in a model of the depression.

STEADY-STATE ARCS

The steady-state electrical behaviour of the DC arc has been well described previously (Bowman *et al.*, 1969; Bowman, 1994), effectively summarizing a large quantity of data from DC electrical arcs in the 1 to 10 kA range. This work provides a description of how the arc voltage varies as a function of arc length and current, for a given set of conditions in the furnace. The model uses measured and extrapolated arc shapes, fitted to calculated plasma conductivities and estimated temperature profiles.

The high-intensity plasma arc has been modelled by Bowman as emanating from a relatively small attachment area on the graphite electrode, and extends down to the surface of the molten bath. This is shown schematically in Figure 1.

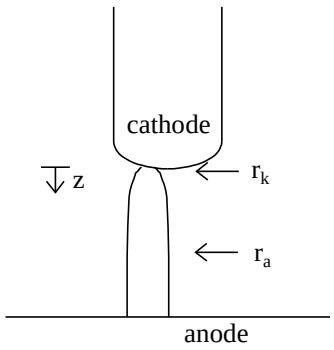

Fig.1 Schematic representation of a DC arc

Equation (1) describes the shape of the conducting volume of the arc as a function of the distance from the cathode attachment spot. The assumptions include an axi-symmetric arc and no interaction effects at the anode.

$$\frac{r_a}{r_k} = 3.2 - 2.2\exp\left(-\frac{z}{5r_k}\right) \qquad (1)$$

The arc radius, r_a, varies with the distance, z, from the cathode surface. The radius, r_k, of the cathode-spot attachment is determined by the value of the cathode-spot current density, estimated by Bowman to be around 3.5 kA/cm^2. Figures 2 and 3 provide a comparison between actual and calculated arc shapes.

Fig.2 4 kA arc in air, struck on a graphite block

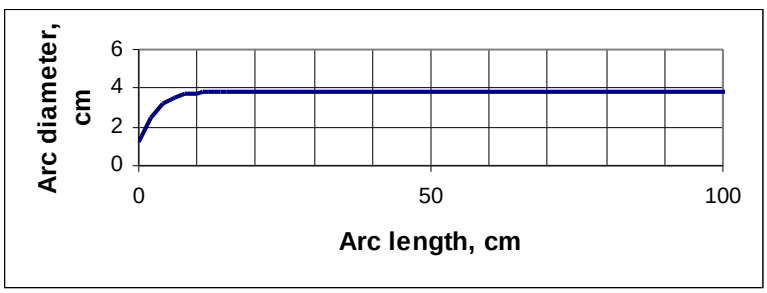

Fig.3 Arc diameter versus length for a 4 kA arc

The arc shape function allows the arc voltage to be obtained by integration. Several constants of Bowman's along with a single variable parameter, the arc resistivity, appear in the arc voltage expression. Variation of the arc resistivity then allows the model to be fitted to pilot or industrial plant data. The integration required is:

$$V = \rho_a \cdot \sqrt{\frac{I \cdot j_k}{\pi}} \cdot \int \left(\frac{r_k}{r_a} \right)^2 dZ \tag{2}$$

$$Z = \frac{z}{r_k} \tag{3}$$

where:
ρ_a – arc resistivity, Ωcm
j_k – cathode-spot current density, kA/cm^2
r_k – cathode-spot radius, cm
r_a – arc radius, cm
I – current, A
V – arc voltage, V
z – axial distance from cathode, cm

The final result of this integration is an expression relating the voltage of the arc to its length and current. This is shown in Equation (4).

$$V_a = \frac{I\rho_a}{m\pi} \left[-\frac{1}{a^2 + ab} + \frac{1}{a^2 + ab.\exp(mL)} + \frac{\ln(a+b)}{a^2} + \frac{mL}{a^2} - \frac{\ln\left[a + b.\exp(mL)\right]}{a^2} \right] \tag{4}$$

$$a = 3.2 r_k \tag{4a}$$

$$b = -2.2 r_k \tag{4b}$$

$$m = \frac{-1}{5 r_k} \tag{4c}$$

$$r_k = \sqrt{\frac{I}{\pi (3500 A/cm^2)}} \tag{4d}$$

where:
V_a – arc voltage, V
I – current, A
ρ_a – arc resistivity, Ωcm
r_k – cathode-spot radius, cm
L – arc length, cm

Equation (4) is depicted graphically in Figure 4, which shows arc voltage as a function of arc length, for a range of different currents, at a given arc resistivity of 0.014 Ωcm.

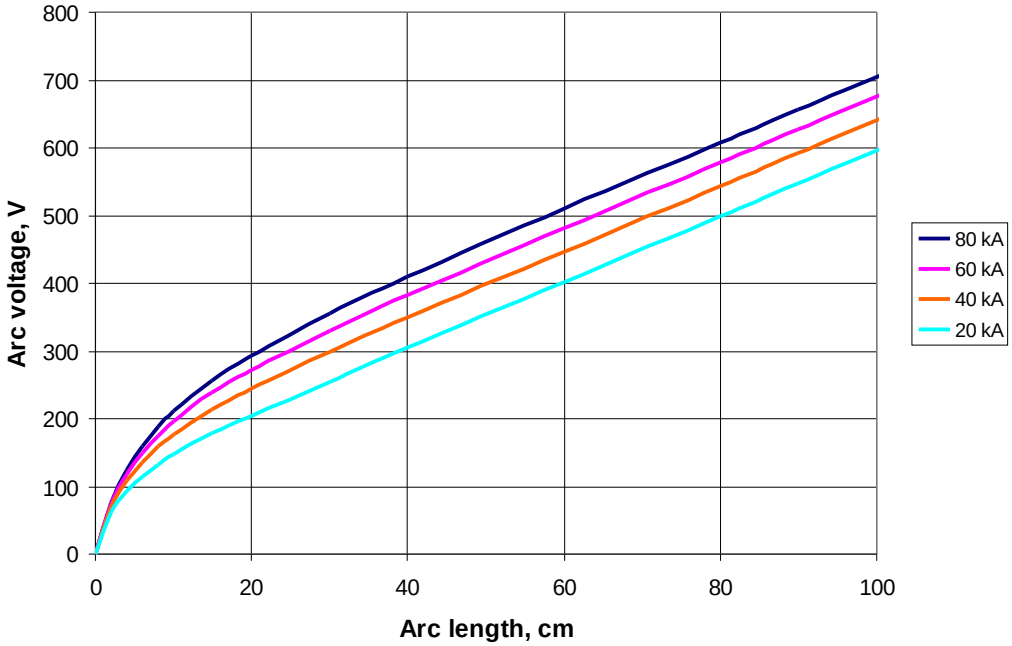

Fig.4 Arc voltage as a function of arc length at different currents, for a given arc resistivity of 0.014 Ωcm

Values for arc resistivity have been obtained experimentally on a number of pilot-plant furnace campaigns at Mintek. These were obtained by measuring the voltage while keeping the current constant and varying the arc length. The value used for the arc resistivity is that which best fits the experimental data. The resistivity varies substantially according to the prevailing gas atmosphere in the furnace. For example, the presence of zinc vapour makes the arc more conductive than carbon monoxide does.

DYNAMIC ARCS

Observations of real arcs (as illustrated in Figures 5 to 9) reveal erratic instabilities and chaotic motion. Sometimes, a helical pattern appears as a precursor to full instability. There are also periods when the arc becomes diffuse and appears to be spread over the entire electrode tip. Clearly, the time-average of this non-steady behaviour has a significant bearing on the properties of the arcs.

Fig.5 Arc about to become unstable

Fig.6 'Pretzel-shaped' arc in air on a graphite block

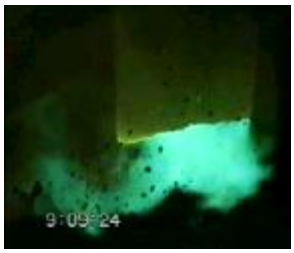

Fig.7
Diffuse 7 kA arc onto slag

Fig.8
Violent splashing at 2 kA

Fig.9
Thicker arc with splashing at 8.1 kA
(Image L16354)

Additional variables come into play when the arc is enclosed in a hot re-radiating furnace vessel, and when the arc is struck on a molten surface that deforms and splashes. The changing shape of the depression in the liquid surface provides a rapidly changing geometrical arrangement that encourages the arc to move to new, shorter, more conductive paths. In moving to a new position, the arc moves extremely rapidly across the tip of the electrode. Figure 10 shows two successive images (one fiftieth of a second apart) in which the arc has moved almost from one side to the other of a 20 cm diameter electrode.

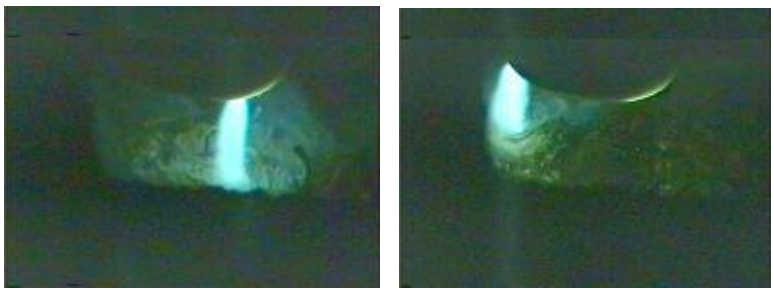

Fig.10 Rapid arc movement in two successive images 1/50 s apart (Images C0935 and C0936)

Multiple 'simultaneous' arcs have been observed and recorded (see Figures 11 and 12), but it would need a higher speed camera to ascertain whether the arcs are truly simultaneous or whether they occurred sequentially during the exposure period, which is usually set to less than 1/50s because of the high intensity of the arc.

Fig.11 Two images (a few minutes apart) showing two arcs 'simultaneously' (Images C0792 and C1225)

Fig.12 Three 'simultaneous' arcs; total current 2 kA

ARC DEPRESSION

The arc jet is seen, from previous measurements and modelling work (Bowman, 1982; Bowman, 1990), to be a high-velocity turbulent self-constricted jet. The force generated by the impingement of such a jet on a dense deformable medium can be very significant, even at pilot-plant scale, and tends to create a cavity at such an interface. The arc-attachment zone (AAZ) is therefore not treated as a flat surface but as a depressed cavity of paraboloidal shape, as suggested by Bowman (1994). The determination of the dimensions of the AAZ depression is aided by an empirical correlation by Maecker (1955) that specifies the dependence of DC arc thrust on current flow. For sufficiently long arcs:

$$T \approx 1.16 \times 10^{-7} . I^2 \tag{5}$$

where:
T – arc thrust, N
I – arc current, A
The volume of the displaced slag, in the paraboloid, may be expressed as:

$$V = \frac{\pi}{2} {r_A}^2 h_A \tag{6}$$

where:
V – volume of paraboloid, m^3
r_A – radius of paraboloid depression, m
h_A – height or depth of paraboloid depression, m

The buoyancy force generated by the absence of the slag from the cavity can be taken as the volume multiplied by the slag density and gravitational acceleration. The buoyancy force may be equated to the thrust, in order to provide an expression relating h_A to r_A.

$$1.16 \times 10^{-7} I^2 = \frac{\pi}{2} \rho g {r_A}^2 h_A \tag{7}$$

where:
ρ - slag density, kg/m^3
g – standard gravitational acceleration, 9.81 m/s^2

One further constraint needs to be imposed on these two dimensions, in order to specify fully the size of the cavity, as a function of the arc current. A relationship between h_A and r_A can either be specified *a priori* or fitted to experimental data. It is understood that the depth cannot reasonably be expected to exceed the diameter of the depression in a stable cavity. Images such as Figure 13 allow one to make a quantitative estimate of the diameter to depth ratio of the arc depression. The images shown in Figure 14 illustrate the different types of depression that may be obtained under different circumstances.

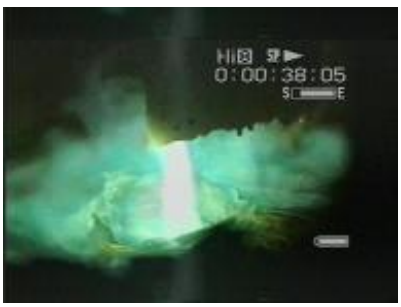

Fig.13 Clear image of arc depression at 2.9 kA (Image F00878)

Fig.14 Arc depressions – punched hole and smeared depression (Images C0833, FL025, FL028)

According to Bowman (1994), depressions in liquids take about 10 to 100 ms to form. Figure 15 shows two depressions existing simultaneously, where the arc has jumped to a new position before the previous depression has had a chance to die away.

Fig.15 Two arc depressions existing simultaneously; 2.6 kA (Image L00683)

ELECTRICAL MODEL OF MOLTEN BATH

In smelting systems, the slag resistance causes a voltage drop across the molten bath. If the slag is highly resistive, this voltage drop can be quite significant.

It is important to have a relatively accurate prediction of the voltage across the slag before specifying the power supply of a new industrial furnace. An incorrect specification can cause the failure of the process, and an over-conservative specification that will guarantee operation over a wide range of conditions may unnecessarily add significantly to the purchase price of the transformer.

The slag bath would be easy to model electrically if it was known to have a flat surface and a uniform conductivity, and if the potential distribution at the upper surface was well understood. A small zone of constant high potential could be envisaged where the arc impinges on the surface, and a zero potential could be envisaged across the bottom surface of the bath where it is in contact with molten metal across the diameter of the furnace. The Laplace equation could then be solved to obtain the potential distribution. However, in reality, the impingement of the arc causes a depression in the surface of the slag. This has to be taken into account in the model, as it can alter the geometrical current distribution quite significantly.

ARCS AT INDUSTRIAL SCALE

The specification of the power supply is one of the principal requirements when an industrial furnace is about to be built, and needs to be in place about twelve to eighteen months before the furnace is to be commissioned. The total power requirement of the furnace is derived from the desired throughput, and the experimentally-determined specific energy requirement for the process. The specification of the operating ranges for voltage and current requires a more detailed understanding of the scale-up of the furnace design. In the past, there has been much speculation about the behaviour of high-current arcs, as some features such as thrust depend on the square of the current. Industrial-scale arcs are very difficult (sometimes even dangerous) to photograph, and in many furnaces, the arc is never visible. Fortunately, video images taken of the high-current arc in an industrial steelmaking furnace showed very similar behaviour to the pilot-scale arcs previously photographed. Some sample images are shown in Figure 16.

Fig.16 Industrial steelmaking arc at 40 kA, 450 V (full power is at 70 kA, 550 V)

ADVANCES IN HIGH-SPEED DIGITAL IMAGING

The work presented here includes a number of images taken using a standard digital still camera as well as with a standard camcorder. Welding filters were used to reduce the intensity of the light to manageable levels. The video images were captured at a rate of 25 frames per second (at a resolution of 768 x 576 pixels), but by separating the odd and even scan lines of the interlaced PAL video image, the frame rate was effectively doubled to 50 frames per second. Much higher filming speeds, with very little delay between successive frames, would be needed in order to capture some of the faster phenomena. High performance digital video cameras may capture images at rates from 1 000 to 60 000 frames per second. This would enable the imaging of phenomena that happen in a millisecond or less to be analysed in detail. Short exposure times permit the digital video camera to capture extremely fast-moving objects on each frame of the video. Classically, high-speed photography used to be performed with the aid of strobe lighting, which gave exposure times down to fractions of a millisecond. With the modern electronics available in high-speed digital video cameras, exposure times of as low as 10 microseconds are available without the need for high-intensity strobes that would otherwise be required to freeze events that are evolving rapidly in time. High-resolution images, up to 1024 x 1024 pixels in size, available in modern CMOS-design digital video cameras, provide sufficient detail for accurate image analysis and tracking of small-scale features from frame to frame.

CONCLUSIONS

A number of critical areas have been identified where an increased understanding is required. The most important of these is the need to better understand the energy transfer in the furnace, closely followed by an ability to correctly specify the requirements of the electrical power supply. Higher-speed digital video imaging would make a valuable contribution towards achieving these objectives.

Dynamic mathematical modelling of arcs is required to better understand the transient phenomena, as the steady-state models do not provide the full picture. Some preliminary work in this area at Mintek has already shown very promising results in using a deterministic model of the arc to predict behaviour that strongly emulates the real chaotic movements of arcs.

The diameter to depth ratio of the arc depression has been determined from photographs, and this has been used for electrical bath modelling.

ACKNOWLEDGEMENT

This paper is published by permission of Mintek.

REFERENCES

Bowman, B., Jordan, G.R., and Fitzgerald, F., 1969. The physics of high-current arcs, *Journal of the Iron and Steel Institute*, June 1969, 798-805.

Bowman, B., 1994. Properties of arcs in DC furnaces, *Electric Furnace Conference Proceedings*, 111-120.

Bowman, B., 1982. MHD effects in arc furnaces, *Symposium on Metallurgical Applications of Magnetohydrodynamics*.

Bowman, B., 1990. Effects on furnace arcs of submerging by slag, *Ironmaking and Steelmaking*, No.2.

Jones, R.T., Barcza, N.A., and Curr, T.R., 1993. Plasma Developments in Africa, Second International Plasma Symposium: World progress in plasma applications, EPRI (Electric Power Research Institute) CMP (Center for Materials Production), Palo Alto, California, 9-11 February 1993 http://www.mintek.co.za/Pyromet/Plasma.htm

Maecker, H., 1955. Plasmastromungen in Lichtbögen infolge eigenmagnetische Kompression, *Z. für Phys.*, Vol.141, 198-216. (Quoted in Bowman, B. Properties of arcs in DC furnaces, *Electric Furnace Conference Proceedings*, 1994, 111-120).